

# Spin gap behaviour in a 2-leg spin-ladder $\text{BiCu}_2\text{PO}_6$

B. Koteswararao,<sup>1</sup> S. Salunke,<sup>1</sup> A.V.Mahajan,<sup>1</sup> I. Dasgupta,<sup>1</sup> and J. Bobroff<sup>2</sup>

<sup>1</sup>*Department of Physics, Indian Institute of Technology Bombay, Mumbai 400076, India*

<sup>2</sup>*Laboratoire de Physique des Solides,*

*Univ. Paris-Sud, 91405 Orsay, France.*

(Date textdate; Received textdate; Revised textdate; Accepted textdate; Published textdate)

## Abstract

We present magnetic susceptibility and heat capacity data on a new  $S = 1/2$  two-leg spin ladder compound  $\text{BiCu}_2\text{PO}_6$ . From our susceptibility analysis, we find that the leg coupling  $J_1/k_B$  is  $\sim 80$  K and the ratio of the rung to leg coupling  $J_2/J_1 \sim 0.9$ . We present the magnetic contribution to the heat capacity of a two-leg ladder. The spin-gap  $\Delta/k_B = 34$  K obtained from the heat capacity agrees very well with that obtained from the magnetic susceptibility. Significant inter-ladder coupling is suggested from the susceptibility analysis. The hopping integrals determined using  $N$ th order muffin tin orbital (NMTO) based downfolding method lead to ratios of various exchange couplings in agreement with our experimental data. Based on our band structure analysis, we find the inter-ladder coupling in the  $bc$ -plane  $J_3$  to be about  $0.75J_1$  placing the compound presumably close to the quantum critical limit.

PACS numbers: 75.10.Pq, 75.40.Cx, 71.20.-b

*Introduction:* Following the discovery of high-temperature superconductivity (HTSC) in the cuprates [1], there has been an increased focus on the properties of low-D antiferromagnetic systems. This is due to the innate exotic properties of these magnetic systems themselves and their supposed connection with HTSC. Significant work has taken place recently elucidating the properties of  $S = 1/2$  and  $S = 1$  Heisenberg chains and their response to impurity substitutions. Whereas quantum fluctuations prevent long-range order (LRO) in 1D Heisenberg systems, 3D systems exhibit conventional LRO. On the other hand, in 2D systems where the strength of magnetic interactions and quantum fluctuations can be comparable, one might expect competing ground states and a quantum critical point separating them. Spin-ladders serve as a bridge between one-dimensional (1D) and two-dimensional (2D) magnetic systems and it is believed that an improved understanding of spin-ladders will lead to a better understanding of magnetism in the 2D systems. A major step was taken in this direction with the prediction of spin-gaps in even-leg ladders and their absence in odd-leg ladders.[2] followed by experimental verification in  $\text{SrCu}_2\text{O}_3$  (2-leg ladder) and  $\text{Sr}_2\text{Cu}_3\text{O}_5$  (3-leg ladder).[3] However, in spite of the large experimental effort, only a small number of gapped ladders have been synthesized and studied. Of these, only two ( $\text{LaCuO}_{2.5}$  and  $\text{Sr}_{14}\text{Cu}_{24}\text{O}_{41}$ ) could be doped significantly with holes of which only the latter becomes superconducting[4]. Some other compounds which have been investigated are  $(\text{C}_5\text{H}_{12}\text{N})_2\text{CuBr}_4$  (Ref. [5]),  $\text{Cu}_2(\text{C}_5\text{H}_{12}\text{N}_2)_2\text{Cl}_4$  (Ref. [6]),  $\text{Cu}_2(\text{C}_5\text{H}_{12}\text{N}_2)_2\text{Br}_4$  (Ref. [7]) which have substantially smaller spin-gaps. There is continued effort to synthesize and study new low-D systems since they provide a rare opportunity to elucidate the significance of low-dimensionality, spin-gap, etc. to HTSC as also allow to examine impurity/doping effects in a strongly correlated cuprate.

In this paper, we report on the preparation and properties of a new cuprate which, we demonstrate, can be modeled as a two-leg ladder system with significant inter-ladder coupling in the  $bc$ -plane and negligible interplanar coupling. The spin-gap, as determined from our susceptibility and heat capacity measurements is about 34 K while the intraladder leg coupling is about 80 K. Our electronic structure calculations within the framework of  $N$ th order muffin tin orbital (NMTO) downfolding method [8] yield hopping integrals between various Cu atoms. Using the NMTO downfolding method, we calculate the Wannier-like effective orbitals which illustrate the shape and extent of the active Cu orbitals and therefore indicate the exchange pathways which lead to the ladder topology. From a practical stand-

point, the estimated  $J/k_B \approx 80$  K provides a unique opportunity to examine the excitations of the coupled ladder system at temperatures ranging from well above  $J/k_B$  to well below  $J/k_B$ . Impurity substitutions will then allow to probe the nature of magnetic effects thus induced, in a wide temperature range.

*Crystal structure and measurements:* Our measurements are on single phase, polycrystalline  $\text{BiCu}_2\text{PO}_6$  samples (space group  $Pnma$  with lattice parameters  $a = 11.776$  Å,  $b = 5.1776$  Å,  $c = 7.7903$  Å).

A schematic diagram of the structure is shown in Fig. 1. The unit cell contains four formula units, with two inequivalent Cu (Cu1 and Cu2) sites and four inequivalent O (O1-O4) sites. The characteristic feature of the structure are  $\text{CuO}_5$  distorted square pyramids, with  $\text{Cu}^{2+}$  ion at the centre of the five fold oxygen co-ordination. Two such pyramids share an edge formed from a pair of basal oxygens (O2) to give rise to a Cu dimer with an intradimer distance of 2.8 Å. Along the  $b$ -axis, each dimer connects two others by its four O1 corners resulting in a zigzag double chain (ladder) running along the  $b$ -axis (see Fig. 1). The interdimer cohesion is further strengthened by  $\text{PO}_4$  tetrahedra that connect two consecutive dimers by O2 corners. The Bi ions are positioned between two ladders. The Cu-O-Cu angle along the leg is about  $112^\circ$  and that along the rung is about  $92^\circ$ . In Fig. 1, various exchange couplings ( $J_1$ ,  $J_2$ , etc.) and hopping integrals ( $t_1$ ,  $t_2$ , etc.) have been indicated.

Our results of the susceptibility  $\chi_{meas}$  (magnetisation  $M$  divided by applied field  $H$ ) as a function of temperature  $T$  using a vibrating sample magnetometer (VSM) of a Physical Property Measurement System (PPMS) from Quantum Design are plotted in Fig. 2. As seen,  $\chi_{meas}$  has a broad maximum around 57 K (indicative of a low-D magnetic system) below which it drops rapidly (suggestive of a spin-gap). A very weak low-temperature upturn is seen below 6.5 K, likely due to extrinsic paramagnetic impurities and/or natural chain breaks in our polycrystalline sample. We now analyse these data quantitatively.

An analytical solution for the spin-susceptibility of two-leg ladders in the full  $T$ -range is not known. However, Johnston, based on extensive quantum Monte Carlo (QMC) simulations[9] has proposed an equation which accurately reproduces the QMC-determined susceptibilities at discrete temperatures. This equation (not reproduced here since it is unwieldy) is useful for determining the exchange couplings by fitting the measured susceptibility data and has been used to analyse such data in the two-leg ladder  $\text{SrCu}_2\text{O}_3$ . We

then fit (dashed line in Fig. 2)  $\chi_{meas}$  to  $\chi_o + C/(T - \theta) + m\chi_{ladder}(T)$  where the fitting parameters are  $\chi_o$ ,  $C$ ,  $\theta$ ,  $J_2/J_1$ ,  $J_1$ , and  $m$ . Here  $\chi_{ladder}(T)$  is the  $\chi$  of isolated ladders as given by Johnston.[9] In the absence of a generic fitting function which can take into account arbitrary inter-ladder interactions, we attempt to do so using the parameter  $m$ . With  $m$  as a variable, the obtained parameters are  $\chi_o = (4.4 \pm 0.1) \times 10^{-4} \text{cm}^3/\text{mol Cu}$ ,  $C = (3.0 \pm 0.2) \times 10^{-4} \text{cm}^3 \text{K}/\text{mol Cu}$ ,  $\theta \sim 0 \text{ K}$ ,  $J_2/J_1 = 0.87 \pm 0.05$ ,  $J_1/k_B = (80 \pm 2) \text{ K}$ , and  $m = 0.41 \pm 0.02$ . The value of the spin-gap using[9]  $\Delta/J_1 = 0.4030(\frac{J_1}{J_2}) + 0.0989(\frac{J_1}{J_2})^3$  is about 34 K. The Curie constant corresponds to less than 0.1 % of isolated  $S = 1/2$  impurities. This value is comparable to typical parasitic Curie terms found in single crystals, indicating the very high quality of our samples. Since the core-diamagnetic susceptibility[10]  $\chi_{core}$  is  $-0.6 \times 10^{-4} \text{cm}^3/\text{mol}$ ,  $\chi_o - \chi_{core}$  yields the Van Vleck susceptibility  $\chi_{VV} = 5 \times 10^{-4} \text{cm}^3/\text{mole}$  which is somewhat higher than  $\chi_{VV}$  of other cuprates. We show in Fig. 2 the curve for isolated 2-leg ladders (with  $J_1/k_B = 80 \text{ K}$ ). We also show the simulated curve for a uniform, 2D  $S = 1/2$  HAF with  $J/k_B = 80 \text{ K}$  where the high- $T$  behavior is generated using the series expansion given by Rushbrooke and Wood.[11] Also, Johnston[12] parametrized the low- $T$  ( $\frac{k_B T}{J} \leq 1$ ) simulations of Takahashi[13] and Makivic and Ding,[14] which we use. The experimental data are lower than both, the 2D HAF curve and the isolated ladder susceptibility. This new behavior points to the importance of a next-near-neighbor (NNN) interaction along the leg (which might be expected due to the zig-zag nature of the leg) which might be frustrating and might even enhance the spin-gap. In a latter section, based on our band-structure calculations, we actually find significant NNN as also inter-ladder couplings. The absence of LRO inspite of these deviations from the isolated ladder picture should motivate the theorists to refine their models of such systems. In the inset of Fig. 2, we plot the normalised susceptibility  $\chi^*(T) = \chi_{spin}(T)J_1/(Ng^2\mu_B^2)$  (where  $\chi_{spin}(T) = \chi_{meas} - \chi_o - C/T$ ) as a function of  $k_B T/J_1$ . We find  $\chi^{*,\text{max}}$  ( i.e.,  $\chi^*$  at the broad maximum) to be about 0.05 which is lower than the expected value for isolated ladders of about 0.12.

To further confirm the spin-gap nature of  $\text{BiCu}_2\text{PO}_6$ , we did heat capacity  $C_p$  measurements. Since the lattice  $C_p$  dominates the data, it has so far not been possible to experimentally determine the magnetic contribution to  $C_p$  in any spin-ladder compound unambiguously. In the present case, we are fortunate to have a non-magnetic analog of  $\text{BiCu}_2\text{PO}_6$  in  $\text{BiZn}_2\text{PO}_6$ . We have then determined the magnetic heat capacity  $C_M$  of  $\text{BiCu}_2\text{PO}_6$  by subtracting the measured  $C_p$  of  $\text{BiZn}_2\text{PO}_6$  from that of  $\text{BiCu}_2\text{PO}_6$  (see Fig. 3

inset). Ours are the first reported  $C_M$  data in a spin-ladder compound. The data are fit to [9]  $C_M(T) = \frac{3}{2}Nk_B \left(\frac{\Delta}{\pi\gamma}\right)^{1/2} \left(\frac{\Delta}{k_B T}\right)^{3/2} \left[1 + \frac{k_B T}{\Delta} + 0.75 \left(\frac{\Delta}{k_B T}\right)^2\right] \exp\left(\frac{-\Delta}{k_B T}\right)$  shown by the solid line (Fig. 3 inset). From the fit, the spin gap  $\frac{\Delta}{k_B} \sim 34$  K, in excellent agreement with our susceptibility results.

*First principles study:* The local density approximation-density functional theory (LDA-DFT) band structure for  $\text{BiCu}_2\text{PO}_6$  is calculated using the linearized-muffin-tin-orbital (LMTO) method based on the Stuttgart TB-LMTO-47 code. [15] The key feature of the non spin-polarized electronic structure presented in Fig. 4 are eight bands crossing the Fermi level which are well separated from rest of the bands. These bands are predominantly derived from the antibonding linear combination of Cu  $d_{x^2-y^2}$  and basal O  $p_\sigma$  states in the local reference frame where the  $z$ -axis is along the shortest Cu-O bond while the  $x$  and  $y$  axes point along the basal oxygens O1 and O2. The band structure is 2D with practically no dispersion perpendicular to the ladder plane (along  $\Gamma X$ ). The eight band complex is half-filled and metallic as expected in LDA. It lies above the other occupied Cu- $d$ , O- $p$ , and Bi- $s$  character dominated bands. The P ( $s, p$ ) and Bi ( $p$ ) derived states are unoccupied and lie above the Fermi level, with the Bi- $p$  states having non-negligible admixture with the conduction bands. This admixture of the conduction band with Bi- $p$  states is important in mediating the Cu-Cu inter-ladder exchange coupling. Starting from such a density functional input we construct a low-energy model Hamiltonian using the NMTO downfolding technique. This method [8] extracts energy selective Wannier-like effective orbitals by integrating out high energy degrees of freedom. The few orbital Hamiltonian is then constructed in the basis of these Wannier-like effective orbitals. Here, we shall retain only Cu  $d_{x^2-y^2}$  orbital in the basis and downfold the rest. The effective Cu  $d_{x^2-y^2}$  muffin tin orbitals generated in the process will be renormalised to contain in their tail other Cu- $d$ , O- $p$ , Bi, and P states with weights proportional to the admixture of these states with Cu  $d_{x^2-y^2}$ . Fourier transform in the downfolded Cu  $d_{x^2-y^2}$  basis gives the desired tight-binding Hamiltonian  $\mathcal{H} = \sum_{\langle i,j \rangle} t_{ij} \left(c_j^\dagger c_i + c_i^\dagger c_j\right)$  in terms of the dominant Cu-Cu hopping integrals  $t_{ij}$ . This tight binding Hamiltonian will serve as the single electron part of the many-body Hubbard model relevant for this system and can be mapped to an extended Heisenberg model with the exchange couplings related to the LDA hoppings by  $J_{ij} = \frac{4t_{ij}^2}{U_{eff}}$  where  $U_{eff}$  is the screened onsite Coulomb interaction. The various hoppings are displayed in Table 1 and indicated in Fig. 1. The intra-dimer (rung) hopping proceeds mainly via the edge sharing oxygens

while the inter-dimer interaction (leg hopping) proceeds via the corner sharing oxygens with support from the  $\text{PO}_4$  complex. As anticipated in the experiments, we do indeed find that the ratio of the rung hopping to the leg hopping  $J_2/J_1 \approx 1$ . We find that the NNN coupling along the leg  $J_4$  is about  $0.3 J_1$ . Depending on the relative sign of this interaction with respect to that of  $J_1$  one might get significant frustration effects which should also have a bearing on the ground state of the system. We also find an appreciable coupling between the ladders ( $J_3/J_1 \approx 0.75$ ) mediated primarily by the unoccupied Bi- $p$  states. Our conclusion is further supported by the plot of the corresponding Cu  $d_{x^2-y^2}$  Wannier function in Fig. 5. We find that each Cu  $d_{x^2-y^2}$  orbital in the unit cell forms strong  $pd\sigma$  antibonding with the neighboring O- $p_x$ /O- $p_y$  orbitals resulting in the conduction band complex. The Cu ions strongly couple along the leg as well as the rung of the ladder confirming the hoppings in either direction should be comparable. The O- $p_x$ /O- $p_y$  tails bend towards the Bi atom, indicating the importance of the hybridization effect from the Bi cations and therefore enhances the Cu-Cu interladder exchange interaction (see table 1).

*Conclusion:* In conclusion, we have presented a new  $S = 1/2$  2-leg ladder  $\text{BiCu}_2\text{PO}_6$ . From our  $\chi$  and  $C_M$  data we obtain a spin-gap  $\Delta/k_B \sim 34$  K and a leg coupling  $J_1/k_B \sim 80$  K. From our first principles LDA-DFT calculations, we find  $J_2/J_1 \sim 1$  and a significant inter-ladder interaction in the corrugated  $bc$ -plane ( $J_3/J_1 \sim 0.74$ ). Considering that the uniform  $S = 1/2$  2D AF system has an ordered ground state, we feel that the strong inter-ladder interaction in  $\text{BiCu}_2\text{PO}_6$  places it close to a quantum critical point. The moderate value of the  $\Delta/k_B$  in  $\text{BiCu}_2\text{PO}_6$  will allow one to explore the magnetic properties in a large  $T$  range, well below and well above the gap temperature, enabling a comparison with and refinement of theoretical models. We feel that there might still be unanticipated features in the physics of low-D magnets and we expect our work to motivate others to carry out numerical simulations and explore the phase-diagram of coupled 2-leg ladders in the presence of NNN couplings along the leg. We are presently considering doping/substitutions in this 2-leg ladder which might be able to tune the inter-ladder exchange and effect a quantum phase transition.

We thank the Indo-French Center for the Promotion of Advanced Research for financial support.

- 
- <sup>1</sup> J. G. Bednorz and K. A. Mueller, *Z. Phys.* **B64**, 189 (1986).
- <sup>2</sup> S. Gopalan, T. M. Rice, and M. Sigrist, *Phys. Rev. B* **49**, 8901 (1994).
- <sup>3</sup> M. Azuma, Z. Hiroi, M. Takano, K. Ishida, and Y. Kitaoka, *Phys. Rev. Lett.* **73**, 3463 (1994).
- <sup>4</sup> E. Dagotto, *Rep. Prog. Phys.* **62**, 1525 (1999).
- <sup>5</sup> B.C.Watson, V.N. Kotov, M.W. Meisel, D.W. Hall, G.E. Granroth, W.T. Montfrooij, S.E. Nagler, D.A. Jensen, R. Backov, M.A. Petruska, G.E. Fanucci, D.R. Talham, *Phys. Rev. Lett.* **86**, 5168 (2001).
- <sup>6</sup> G. Chaboussant, P.A. Crowell, L.P. Lévy, O. Piovesana, A. Madouri, D. Maily, *Phys. Rev. B* **55**, 3046 (1997).
- <sup>7</sup> H. Deguchi, S. Sumoto, S. Yamamoto, S. Takagi, H. Nojiri, and M. Motokawa, *Physica B* **284-288**, 1599 (2000).
- <sup>8</sup> O.K. Andersen and T. Saha-Dasgupta, *Phys. Rev B* **62**, R16219 (2000).
- <sup>9</sup> D. C. Johnston, M. Troyer, S. Miyahara, D. Lidsky, K. Ueda, M. Azuma, Z. Hiroi, M. Takano, M. Isobe, Y. Ueda, M.A. Korotin, V.I. Anisimov, A.V. Mahajan, and L.L. Miller, unpublished, cond-mat/0001147.
- <sup>10</sup> P.W. Selwood, *Magnetochemistry*, Interscience, New York, 1956.
- <sup>11</sup> G. S. Rushbrooke and P. J. Wood, *Molec. Phys.* **1**, 257 (1958).
- <sup>12</sup> D. C. Johnston, *Handbook of Magnetic Materials*, edited by K. H. J. Buschow (Elsevier Science Publishers B. V., Amsterdam, 1997).
- <sup>13</sup> M. Takahashi, *Phys. Rev. B* **40**, 2494 (1989).
- <sup>14</sup> M. S. Makivic and H.-Q. Ding, *Phys. Rev. B* **43**, 3562 (1991).
- <sup>15</sup> O. K. Andersen, *Phys. Rev. B*, **12** 3060 (1975); O. K. Andersen and O. Jepsen, *Phys. Rev. Lett.* **53**, 2571(1984); O. K. Andersen and O. Jepsen, The STUTTGART TB-LMTO program, version 47, (2000).

### Table Caption

Table 1 Hopping parameters ( $t_n$ ) between various Cu's are tabulated along with the corresponding Cu-Cu distances. The hopping paths are indicated in Fig. 1.

Hopping path	Cu-Cu distance	$t_n$	$J_n/J_1$
	in Å	in meV	$= (t_n/t_1)^2$
leg ( $t_1$ )	3.22	155	1
rung ( $t_2$ )	2.90	154	1
inter-ladder ( $t_3$ )	4.91	133	0.74
NNN in leg ( $t_4$ )	5.18	91	0.34
diagonal ( $t_{5A}$ )	4.43	30	0.04
diagonal ( $t_{6A}$ )	5.81	26	0.03

Figure captions

Fig. 1 (Color Online) A schematic of the  $\text{BiCu}_2\text{PO}_6$  crystal structure is shown. It can be seen that 2-leg ladders run along the crystallographic  $b$ -direction. The 2-leg ladder is separately shown for clarity. Also shown are the various significant hopping parameters/exchange couplings between Cu atoms.

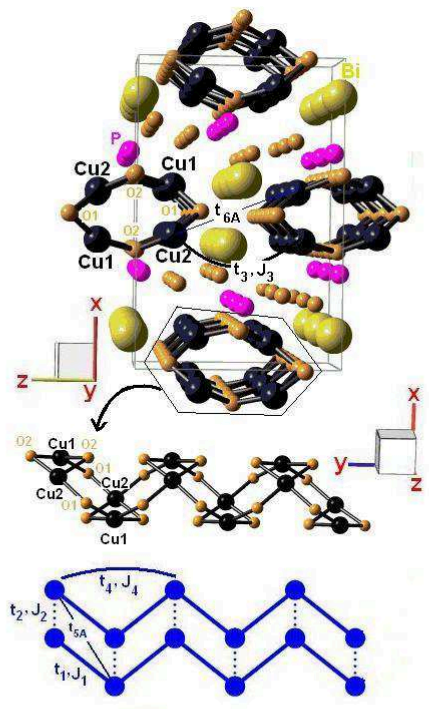
Fig. 2 (Color Online) Magnetic susceptibility ( $\chi_{meas} = M/H$ ) vs. temperature  $T$  for  $\text{BiCu}_2\text{PO}_6$  in an applied field of 5 kG. The open circles represent the raw data and the dashed line is a fit (see text). Also shown are simulated curves for the isolated ladder (dark gray line) and for the 2D HAF (gray line). The inset shows the dependence of  $\chi^*$  on  $k_B T/J_1$  (see text).

Fig. 3 (Color Online) The measured heat capacity as a function of  $T$  for  $\text{BiCu}_2\text{PO}_6$  and  $\text{BiZn}_2\text{PO}_6$ . Inset: the magnetic specific heat of  $\text{BiCu}_2\text{PO}_6$  along with a fit (see text).

Fig. 4 (Color Online) LDA band dispersion of  $\text{BiCu}_2\text{PO}_6$  along various symmetry directions.

Fig. 5 (Color Online) Effective Cu1  $d_{x^2-y^2}$  orbital with lobes of opposite signs colored as black and white. The  $d_{x^2-y^2}$  orbital is defined with the choice of local coordinate system as discussed in the text (height of the isosurface =  $\pm 0.09$ ). The spheres represent the ions.





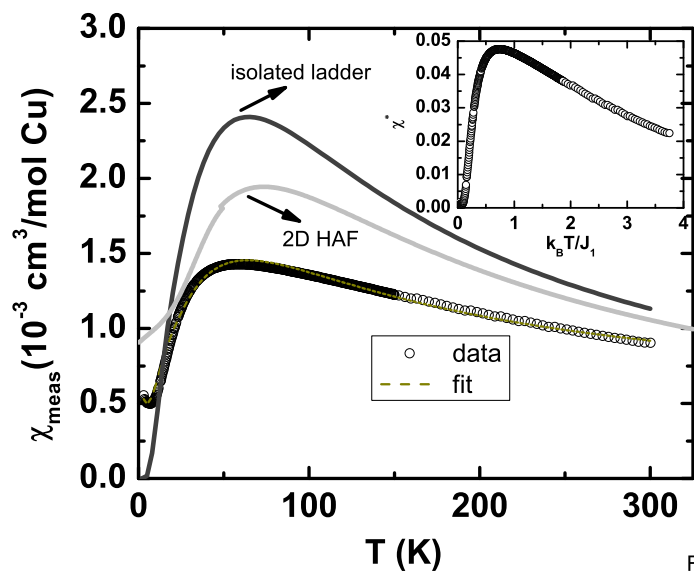


Fig. 2

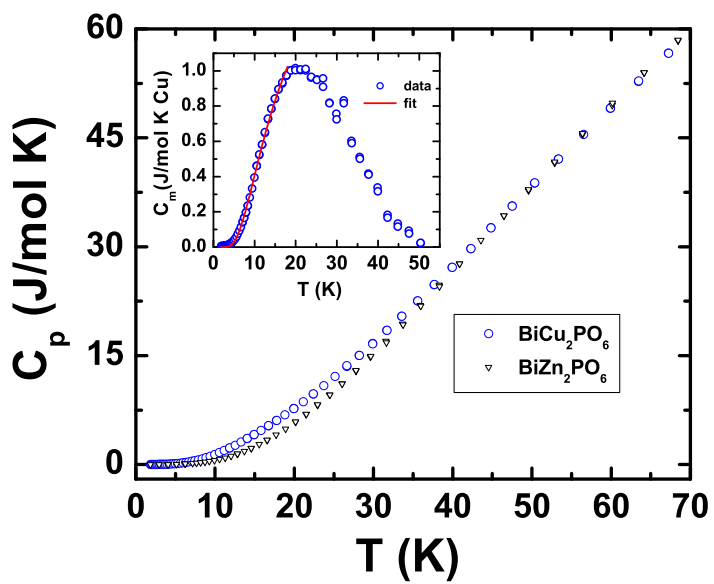


Fig. 3

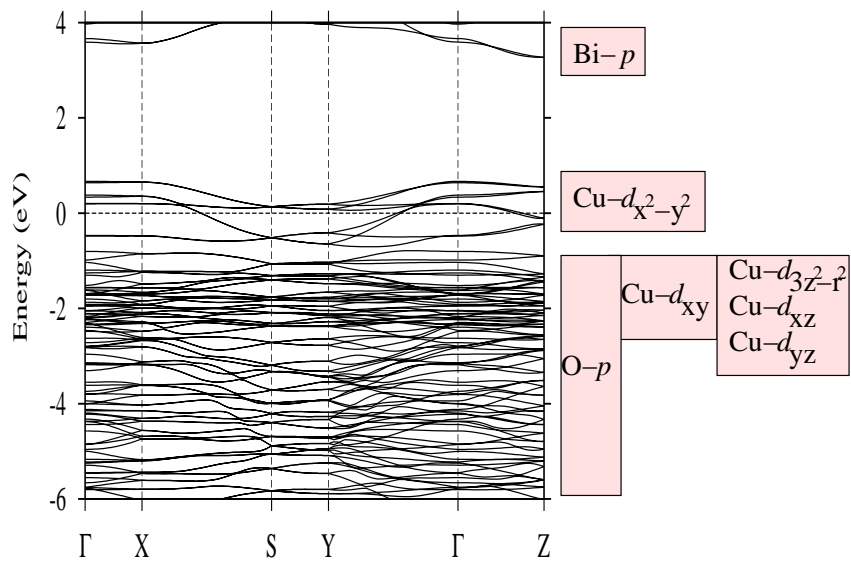


Fig. 4

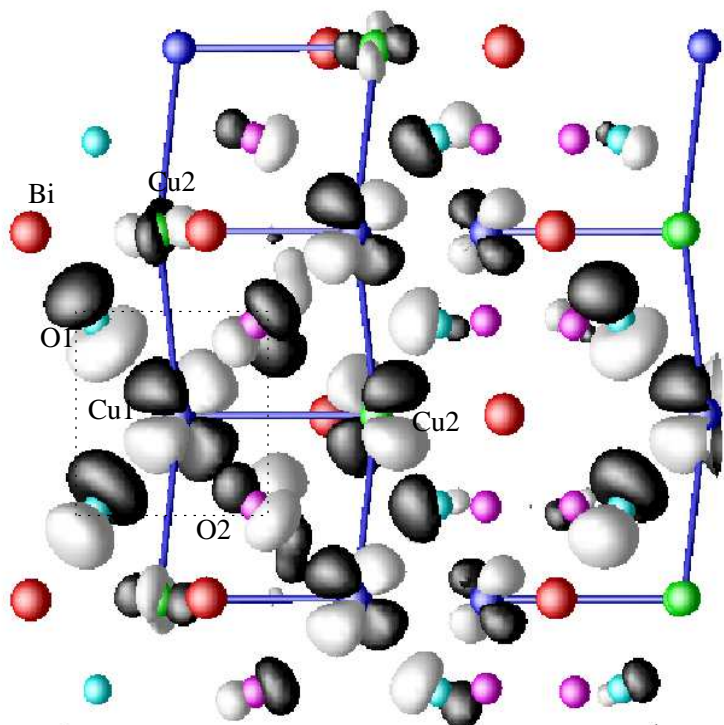


Fig. 5